ISSN 1024-8560, Atmospheric and Oceanic Optics, 2021, Vol. 34, No. 6, pp. 567–576. © Pleiades Publishing, Ltd., 2021.
Russian Text © The Author(s), 2021, published in Optika Atmosfery i Okeana.

OPTICS OF CLUSTERS, AEROSOLS, AND HYDROSOLES

Change in the Air Composition upon the Transition from the Troposphere to the Stratosphere

P. N. Antokhin[a], V. G. Arshinova[a], M. Yu. Arshinov[a], B. D. Belan[a, *], S. B. Belan[a], L. P. Golobokova[b], D. K. Davydov[a], G. A. Ivlev[a], A. V. Kozlov[a], A. S. Kozlov[c], V. I. Otmakhov[d], T. M. Rasskazchikova[a], D. V. Simonenkov[a], G. N. Tolmachev[a], and A. V. Fofonov[a]

[a] *V.E. Zuev Institute of Atmospheric Optics, Siberian Branch, Russian Academy of Sciences, Tomsk, 634055 Russia*

[b] *Limnological Institute, Siberian Branch, Russian Academy of Sciences, Irkutsk, 664033 Russia*

[c] *Voevodskii Institute of Chemical Kinetics and Combustion, Siberian Branch, Russian Academy of Sciences, Novosibirsk, 630090 Russia*

[d] *National Research Tomsk State University, Tomsk, 634050 Russia*

**e-mail: bbd@iao.ru*

Received September 29, 2021; revised September 29, 2021; accepted October 5, 2021

Abstract—Airborne sensing data are used to study the change in the air composition upon the transition from the troposphere to the stratosphere. The distribution of seven gases and the size spectrum and chemical composition of aerosol particles are analyzed. It is shown that when crossing the tropopause, the concentrations of H_2O, CO, and CH_4 sharply decrease, while the concentrations of O_3 and NO_2 and the aerosol particle number density, to the contrary, increase. Above the tropopause, Si predominates in the elemental composition and SO_4^{2-} prevails in the ionic composition. In the troposphere, terrigenous elements Al, Cu, and Fe predominate, while in the ionic composition the prevailing set of several ions varies from one region to another. Noticeable differences in the size spectrum of particles are revealed as well.

Keywords: atmosphere, aerosol, air, vertical distribution, gases, composition, stratosphere, troposphere

DOI: 10.1134/S1024856021060300

INTRODUCTION

The stratosphere and troposphere are the main atmospheric layers that determine a significant part of atmospheric processes on our planet. They are separated by the tropopause, i.e., a stably stratified layer which hinders the air exchange between the stratosphere and the troposphere [1]. As a result, the air composition in the stratosphere and troposphere is somewhat different [2–4]. However, the tropopause is not impenetrable; therefore, there is an exchange of atmospheric constituents between the both layers. The very detailed overview of such processes is given in [5]. The exchange intensifies in the zone of large-scale synoptic objects [6–8], especially in high-altitude frontal zones, the so-called tropopause folds [9–11]. In regions not involved in dynamic distortions, the exchange intensity is minimal.

Under the conditions of changing climate, the air composition in the troposphere has noticeably changed. As shown in [12], this affected the characteristics of the troposphere and stratosphere. Since 1980 till 2018, the tropopause rose by an average of 150 m, and the stratopause dropped by 400 m. It is predicted the stratopause will descend by 1.3 km that by 2080. Consequently, the exchange processes between the troposphere and stratosphere should also change. For example, the tropopause height well correlates with the height of the ozonopause [13] which determines the ozone transport from the stratosphere to the troposphere [14]. Thus, the exchange of substances will affect the air composition both in the troposphere and in the stratosphere and, accordingly, their radiative conditions.

As noted in [15], there is no technique for retrospective analysis similar to the use of paleoclimatic data. Therefore, it is necessary to study the processes of air exchange between the troposphere and the stratosphere under the warming climate, especially if we take into account that one of geoengineering methods for influencing climate-forming factors is connected with the introduction of an additional amount of aerosols into the stratosphere [16].

There are relatively few studies concerning the redistribution of gaseous constituents and aerosol between the troposphere and stratosphere. In [17, 18], the attention is paid to the importance of the water vapor transfer through the tropopause to the stratosphere. An increase in the water vapor can intensify

Table 1. Equipment mounted in the flying laboratory and its technical characteristics

Unit	Device/sensor	Measured parameter	Range	Error
Gas-analysis system	G2301-m	CO_2, ppm	0–1000	<0.2 ppm
		CH_4, ppm	0–20	<0.0015 ppm
		H_2O, ppm	0–70000	<150 ppm
	TEI Model 49C	O_3, ppm	0–200	0.001 ppm
	TEI Model 48C	CO, ppm	0–1000	±1%
	TEI Model 42*i*	NO/NO_2, μg/m^3	0–10/500	±1%
Aerosol system	GRIMM #1.109	D_p, μm (31 channels) N, cm^{-3}	0.25–32 0–2000	– ±3%
	Diffusion aerosol spectrometer	D_p, nm (20 channels) N, cm^{-3}	3–200 0–500000	– ±10%

ozone depletion by human-made ozone-depleting substances and thus trigger an increase in ultraviolet radiation on the Earth's surface. Measurement and simulation results [19, 21] show a decrease in the water vapor concentration down to 2–4 ppm upon the transition from the troposphere to the stratosphere. Since ozone is formed in large quantities in the stratosphere, its concentration above the tropopause rapidly increases with altitude and reaches a maximum at a level of 20–25 km depending on the geographical latitude [22–24]. In addition to water vapor and ozone, the methane [21] and carbon monoxide [25, 26] concentrations were also measured, which decreased with altitude above the tropopause.

To replenish the data on the change in the air composition upon the transition from the troposphere to the stratosphere, in this work, we analyze the vertical distribution of seven gases and aerosols at the tropopause level and in the adjacent layers based on airborne sensing data.

EXPERIMENTAL

For the study, we used the data of airborne sensing obtained with the Optik Tu-134 flying laboratory described in [27]. Since the laboratory equipment has been significantly updated, Table 1 shows the characteristics of the devices used in the experiments.

In addition to the devices tabulated, aspiration units were used for collecting samples onto filters in order to determine the chemical composition of aerosol. To study the inorganic component, the aerosol was sampled on AFA-ChA-20 filters. The elemental composition was determined by atomic emission spectral analysis [28, 29], while the ionic composition was determined by the ion chromatography [30, 31].

Flights, in which the flying laboratory crossed the tropopause, were included in the analysis. The tropopause was determined from the temperature gradient (up to 2°C/km) (this tropopause is called thermal [32]). There were 14 such cases. Three of them, where all the gaseous constituents and aerosol were measured, were performed in September 2020, and eleven, with an incomplete set of measured constituents, in October 2014. All the selected profiles were recorded over the Arctic seas or coastal territories. This is not surprising, since the tropopause in the northern latitudes is much lower than in the midlatitudes [33].

The tropopause was crossed in horizontal flights through high-altitude frontal zones (Figs. 1a and 1b), as well as during vertical sensing at centers of deep cyclones (Fig. 1c) or wide troughs (Fig. 1d). In the first case, the slope of the tropopause took place [34]. In the second case, it was "pulled" down at the center of a cyclone [35].

RESULTS AND DISCUSSION

The analysis has shown that all the measured constituents can be divided into three groups according to the character of variations in the concentration upon the transition through the tropopause: (1) H_2O, CO, and CH_4 (Table 2), the concentrations of which sharply decreased in the stratosphere in all the cases; (2) O_3 and NO_2, the concentrations of which, to the contrary, increased when crossing the tropopause, along with the aerosol particle number density (N); (3) NO and CO_2, concentrations of which could both decrease and increase; sometimes they showed the neutral behavior.

Figures 2–4 show how the concentrations of atmospheric constituents vary when crossing the tropopause.

It can be seen from Fig. 2a that the specific humidity decreases with altitude up to the tropopause level and then slightly increases. This character of the variation is quite natural keeping in mind the physical properties of moisture content in the atmosphere [36],

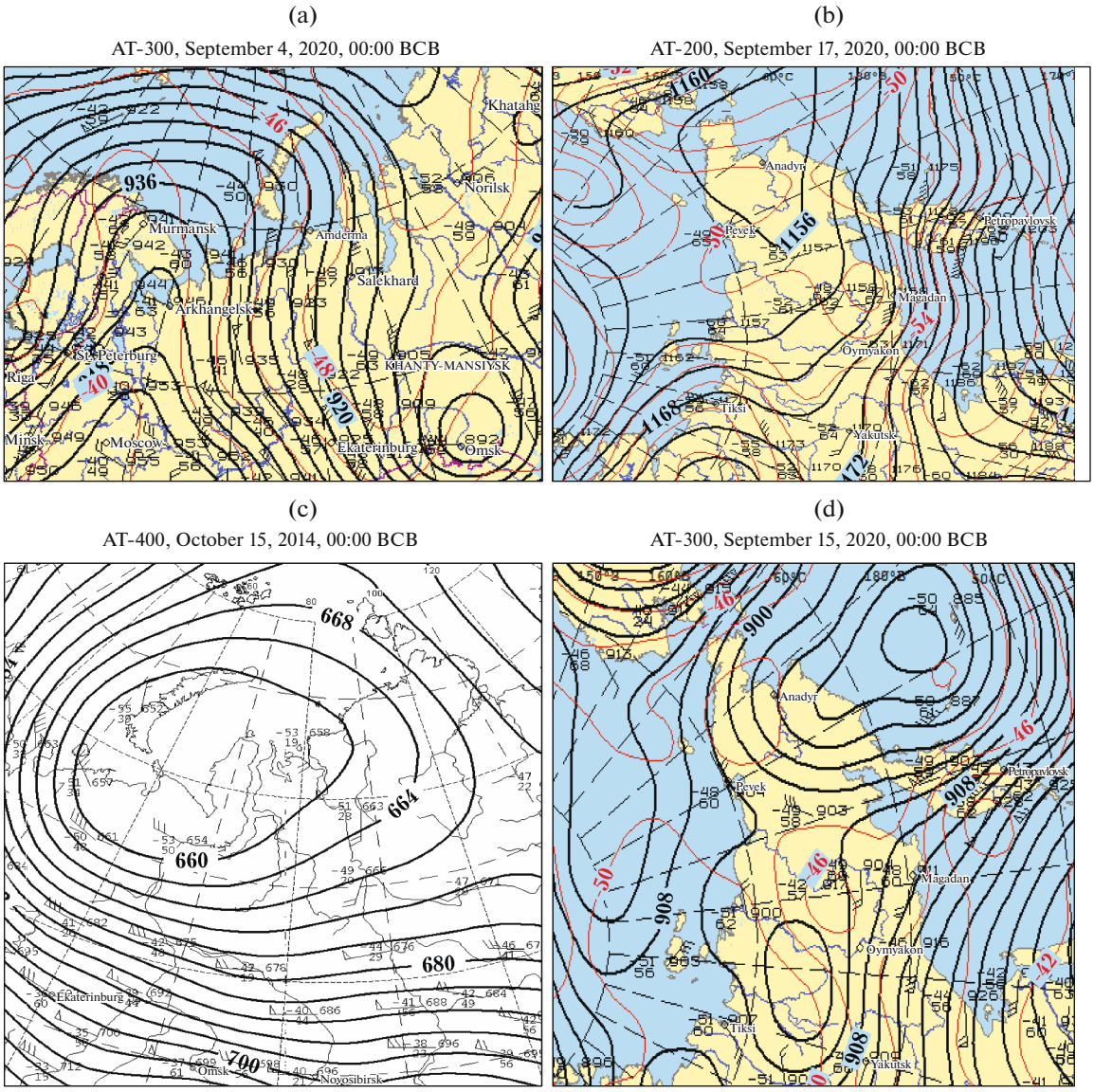

Fig. 1. Baric topography maps for regions where the tropopause was crossed.

since the maximal concentration of water vapor in air exponentially decreases with the temperature. As for the absolute values, the specific humidity shown in Fig. 2 it is much higher than that observed in [19–21]. Two explanations are possible here. The first one is that low values of the specific humidity are close to the threshold and measurement error of the gas analyzer used. The second explanation is that the measurements have been carried out in the lowest part of the stratosphere, where water vapor inflows from the troposphere.

A sharp drop in the concentration upon the transition from the troposphere to the stratosphere is also

Table 2. Character of change in the concentration of air constituents when crossing the tropopause

Character of change	H_2O	O_3	N	CO	CH_4	CO_2	NO_2	NO
Growth	–	14	11	–	–	6	3	3
Drop	14	–	1	14	14	6	–	–
Neutral	–	–	2	–	–	2	–	–

N is the particle number density; $d > 0.25$ μm.

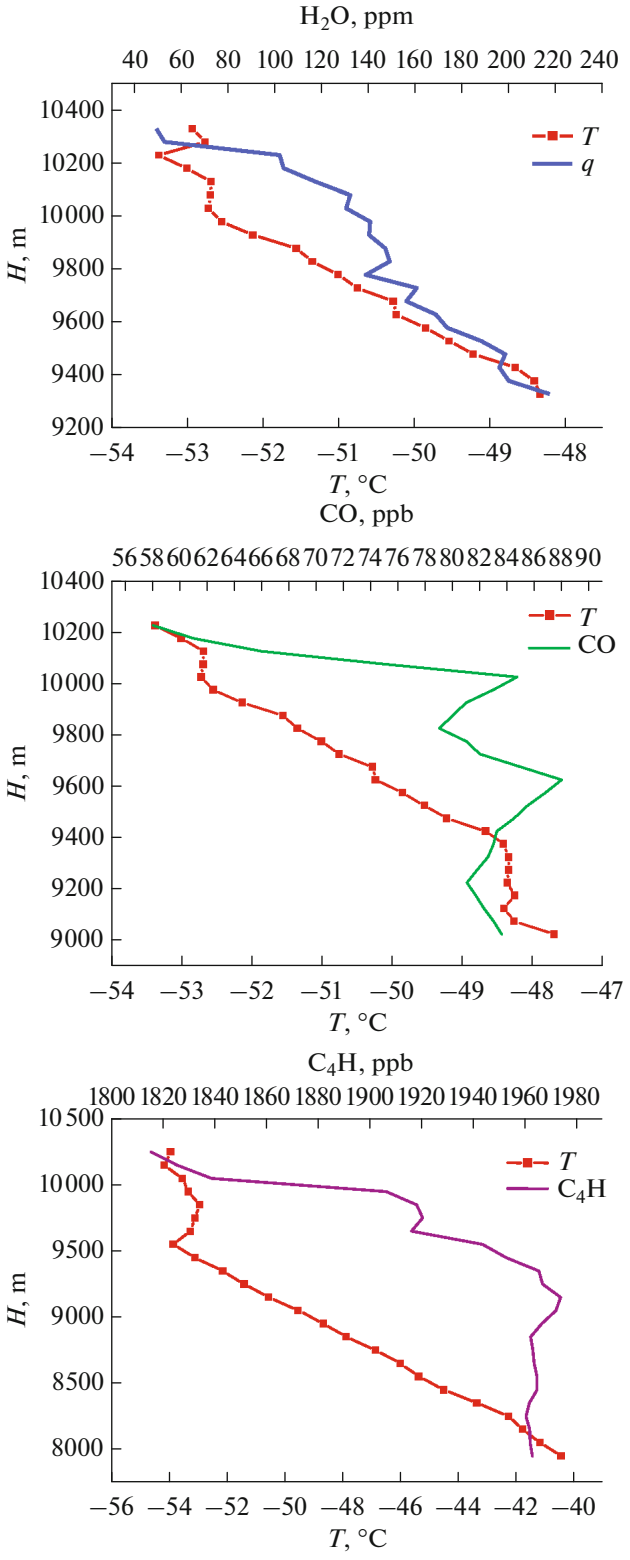

Fig. 2. Vertical distribution of specific humidity, CO, and CH_4 in the tropopause layer.

observed for CO and CH_4 (Figs. 2b and 2c). Similar facts and the values close to the data in Figs. 2a and 2b were also recorded by other research groups [21, 37–39]. A possible reason for the rapid decrease in CO and CH_4 in the stratosphere is considered to be their oxidation by ozone and hydroxyl, whose concentrations here are much higher than in the troposphere [40, 41].

Figure 3 shows that the O_3 and NO_2 concentrations and the aerosol particle number density increase upon the transition into the stratosphere. If the increase in the O_3 and NO_2 is quite clear (they are formed in the stratosphere in photochemical cycles [42, 43]), then the reason for the increase in the number of particles is not clear yet. We will return to this issue a little later.

Let us dwell on the issue of the variable character of the variation in the CO_2 concentration in the tropopause layer (Table 2, Fig. 4).

One can see from Fig. 4a that the carbon dioxide concentration started to increase in the troposphere and continued to grow in the stratosphere. An opposite pattern can be seen in Fig. 4b: the CO_2 concentration varies in the troposphere and decreases in the stratosphere. However, the amplitudes of the variations are small (2–3 ppm). The data of Table 2 indicate that variations in the both directions are equally probable. The similar fact was also noticed in [38], where the different character of variations in carbon dioxide and oxide was explained by the territory, where the airborne sensing was carried out, as follows. A barrier arises between the polar dome and the midlatitudes. When sensing to the south of the dome, the concentration should increase due to inflow of enriched continental air masses. The profile inside the dome should show a decrease, because of lower content of the atmospheric constituents there. Our attempt to check this conclusion failed. It is possible that the boundary of the polar dome was much farther north during our experiments.

We succeeded in collecting aerosol samples in the stratosphere in three cases. The results of comparison of the elemental and ionic compositions for the stratosphere and troposphere are shown in Figs. 5 and 6, respectively. Tropospheric samples were taken 1 km below the tropopause.

It can be seen from Fig. 5 that the elemental composition of aerosol significantly differs in the troposphere and the stratosphere. In addition to the elements shown in Fig. 5, Ca, Mg, and Ti were determined in the composition of aerosol particles. However, their content turned out to be at the level of blank samples, which did not allow their reliable quantitative estimation in the composition of aerosol. The detailed analysis of Fig. 5 is hardly possible. A characteristic feature can be distinguished: Si predominates in the composition of particles in the stratosphere, while Fe or aluminum predominates in the composition of tropospheric particles. The most probable reason for this difference is the long stratospheric lifetime of volcanic eruption products with silicates predominating in their composition [44], while the lifetime of these particles in the troposphere is

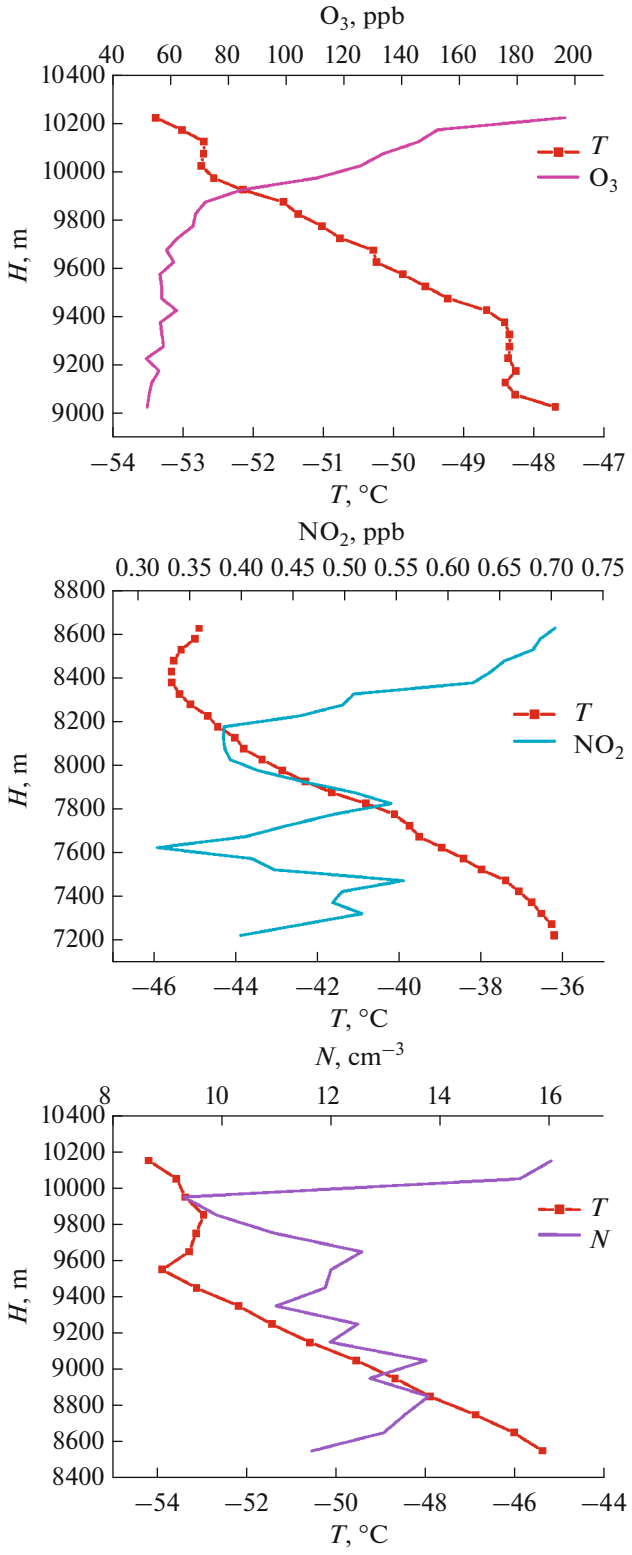

Fig. 3. The same as in Fig. 2, but for O_3, NO_2, and the number density of aerosol particles with $d > 0.25$ μm.

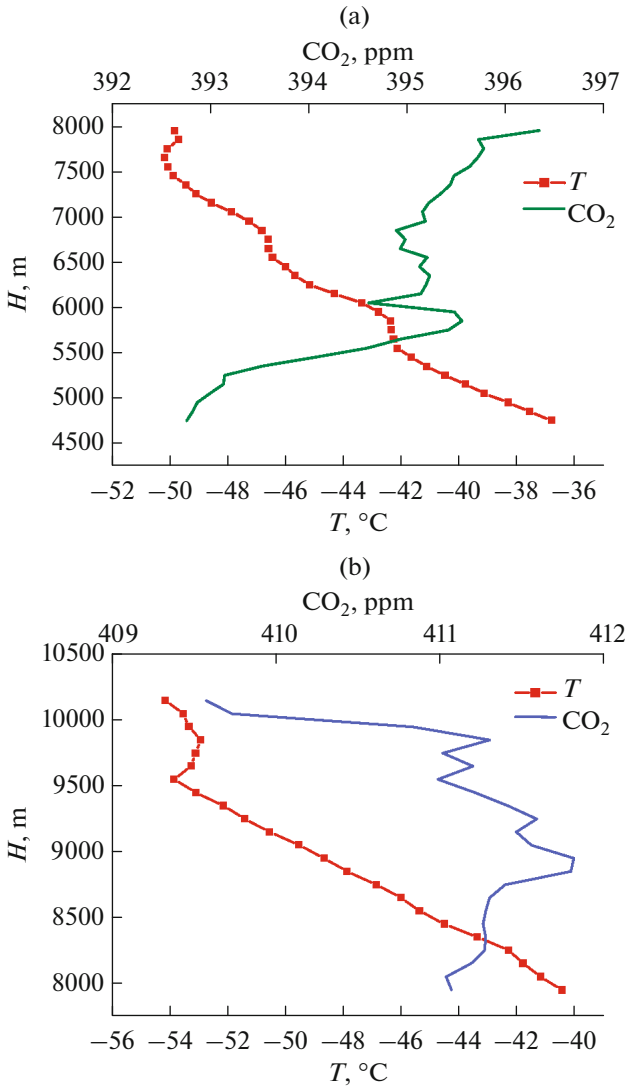

Fig. 4. The same as in Fig. 2, but for CO_2: (a) Kara Sea, October 15, 2014; (b) Arkhangelsk, September 4, 2020.

much shorter. To be noted in the low stratospheric concentration of Be, which is one of the indicators of air mass origin [45]. This is possibly a consequence of the period of measurements: the measurements were carried out in the fall, when the concentration of beryllium in the atmosphere is minimal [46].

Significant differences between stratospheric and tropospheric aerosols were also found in the ionic composition (Fig. 6).

Figure 6 shows that sulfate aerosol based on the SO_4^{2-} ion predominates in the stratosphere. Ions of terrigenous origin prevail in the troposphere. This is in a good agreement with the earlier data [44]. Some of the ions shown in Fig. 6 were also found in the stratosphere in the special experiments [47, 48].

These differences in the chemical composition of aerosol certainly affect the particle size distribution. The complete spectra of these distributions are shown in Fig. 7 (on the log scale). Since the system for measuring the particle size distribution consisted of two devices with different operation rates, and the time of

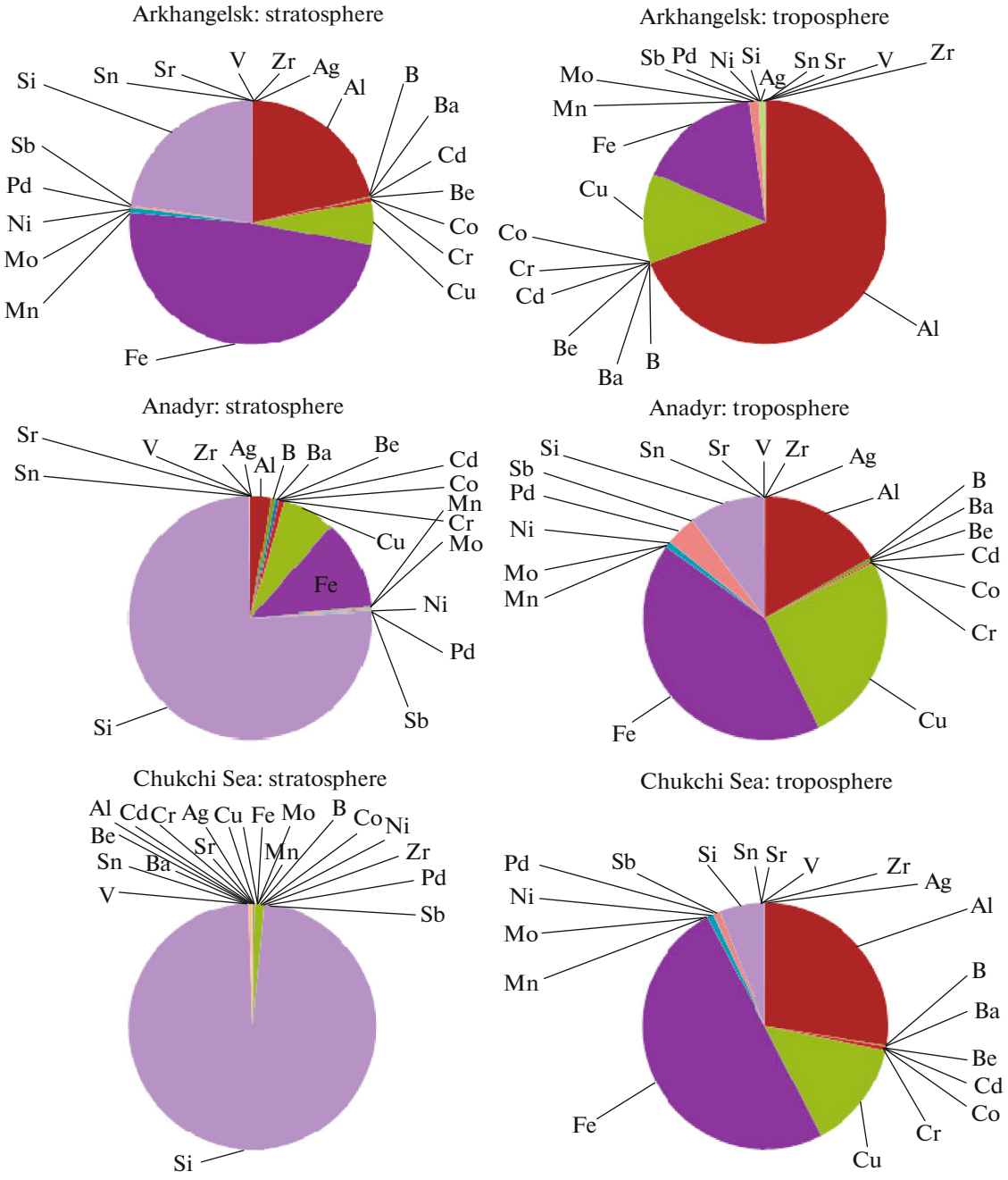

Fig. 5. Elemental composition of aerosol in the stratosphere and troposphere.

horizontal flights was only few minutes, it was difficult to find the periods when the readings were carried out synchronously. That is why there are a few data on the complete size distribution of aerosol particles. Two spectra were obtained for the regions near Arkhangelsk and Anadyr. An altitude of about 9 km, i.e., under the tropopause, was taken as control for the stratosphere.

Figure 7 shows that the maximal particle number densities in both the troposphere and the stratosphere fall on the Aitken mode (20–50 nm). The differences in the particle size distributions in the stratosphere and the troposphere are noticeable. It can be noted that the both distribution spectra are slightly shifted to the right, toward the range of larger particles, in the stratosphere. The stratosphere contains more coarse particles ($d > 1$ μm).

In the both cases, the stratosphere contains particles of the nucleation mode (3–20 nm). This indicates that, despite the low humidity and the very low content of ammonia, new particles form in the stratosphere. As can be judged from the predominance of SO_4^{2-} in the ionic composition (Fig. 6), particles are

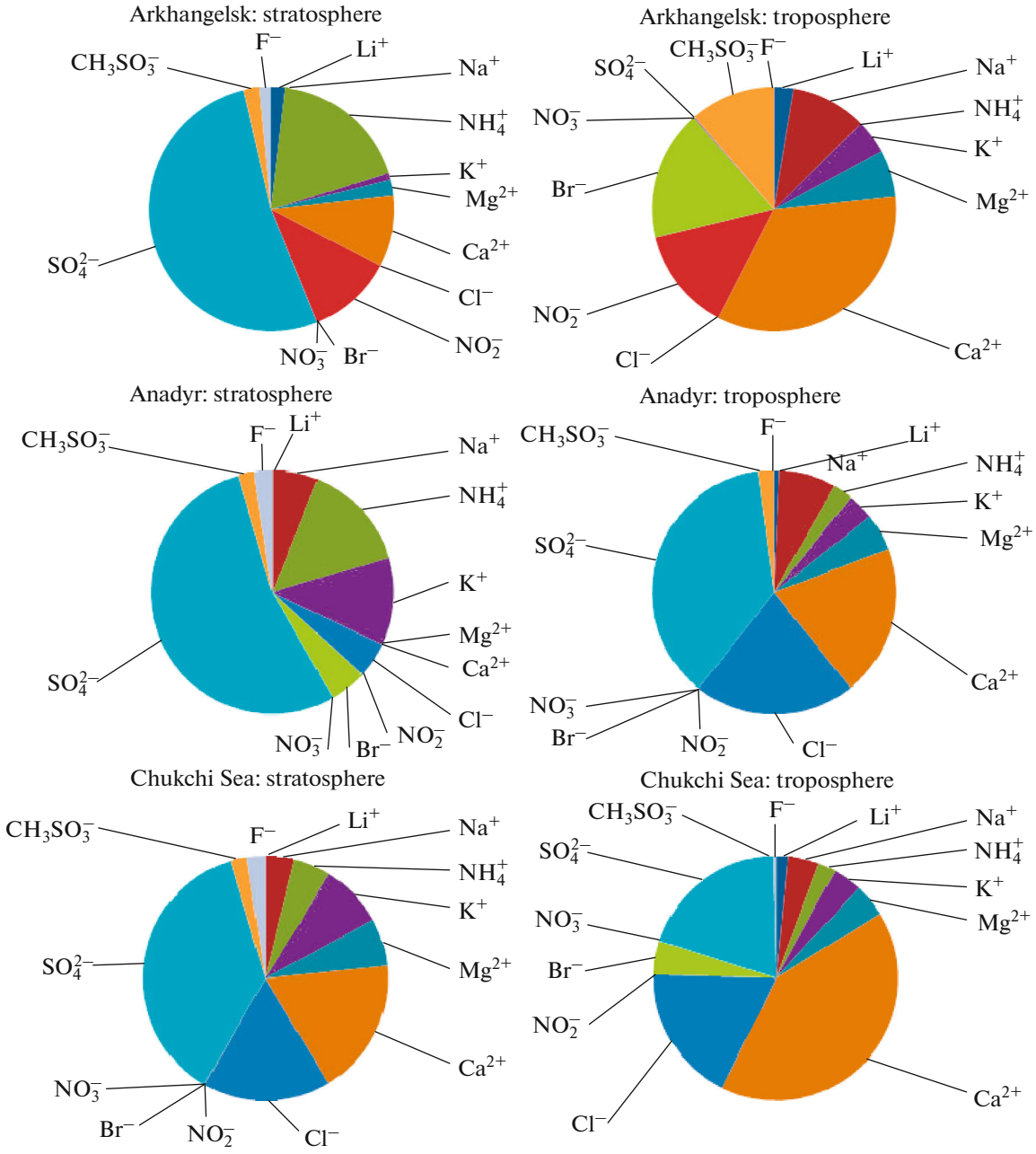

Fig. 6. Ionic composition of aerosol in the stratosphere and troposphere.

generated by the sulfuric acid mechanism. This likely explains the increase in the particle number density above the tropopause, as shown in Fig. 3.

These results obtained from the analysis of few cases should be considered preliminary.

CONCLUSIONS

The air composition considerably changes upon the transition from the troposphere to the stratosphere. The concentration of such gases as H_2O, CO, and CH_4 sharply decreases above the tropopause. The aerosol particle number density and the concentrations of O_3 and NO_2, to the contrary, increase above this layer. The carbon dioxide concentration may increase and decrease with equal probability. For NO, no unambiguous trend was found due to its low content at these altitudes.

The chemical composition of aerosol also significantly differs in the stratosphere and the troposphere. Above the tropopause, Si predominates in the elemental composition and SO_4^{2-} prevails in the ionic composition. In the troposphere, terrigenous elements Al,

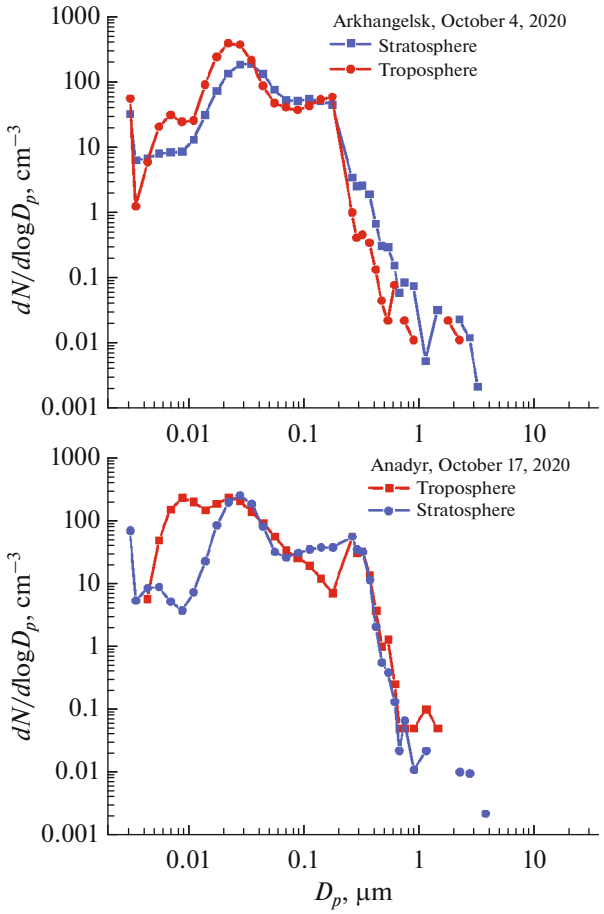

Fig. 7. Aerosol particle size distribution in the stratosphere and troposphere.

Cu, and Fe predominate in the elemental composition, and a set of several ions, varying from one region to another, predominates in the ionic composition.

There are also differences in the size spectrum of aerosol particles. In the stratosphere, the size distribution curve is generally shifted to the right, reflecting the longer age of the particles.

ACKNOWLEDGMENTS

This study is based on the data obtained with the Tu-134 Optik flying laboratory being a part of the Atmosfera Common Use Center.

FUNDING

The work is supported by the Ministry of Science and Higher Education of the Russian Federation (agreement no. 075-15-2021-934).

CONFLICT OF INTEREST

The authors declare that they have no conflicts of interest.

REFERENCES

1. Z. M. Makhover, *Climatology of the Tropopause* (Gidrometeoizdat, Leningrad, 1983) [in Russian].
2. T. Trickl, H. Vogelmann, H. Giehl, H.-E. Scheel, M. Sprenger, and A. Stohl, "How stratospheric are deep stratospheric intrusions?," Atmos. Chem. Phys. **14** (18), 9941–9961 (2014).
3. T. Trickl, N. Bartsch-Ritter, H. Eisele, M. Furger, R. Mucke, M. Sprenger, and A. Stohl, "High-ozone layers in the middle and upper troposphere above Central Europe: Potential import from the stratosphere along the subtropical jet stream," Atmos. Chem. Phys. **11** (17), 9343–9366 (2011).
4. A. A Kukoleva, "Estimation of ozone fluxes across the tropopause within high frontal zones in the Northern Hemisphere," Izv., Atmos. Ocean. Phys. **38** (3), 333–343 (2002).
5. A. R. Ivanova, "Stratosphere-troposphere exchange and its specific features at extratropical latitudes," Rus. Meteorol. Hydrol. **41** (3), 170–185 (2016).
6. A. A. Krivolutsky and A. A. Kukoleva, "Results of Russian investigations into the middle atmosphere (2011–2014)," Izv., Atmos. Ocean. Phys. **52** (5), 497–511 (2016).
7. A. C. Boothe and C. R. Homeyer, "Global large-scale stratosphere-troposphere exchange in modern reanalyses," Atmos. Chem. Phys. **17** (9), 5537–5559 (2017).
8. T. Runde, M. Dameris, H. Garny, and D. E. Kinnison, "Classification of stratospheric extreme events according to their downward propagation to the troposphere," Geophys. Rev. Lett. **43** (12), 6665–6672 (2016).
9. M. Mihalikova, S. Kirkwood, J. Arnault, and D. Mikhaylova, "Observation of a tropopause fold by MARA VHF wind-profiler radar and ozonesonde at Wasa, Antarctica: Comparison with ECMWF analysis and a WRF model simulation," Ann. Geophys. **30** (9), 1411–1421 (2012).
10. M. Mihalikova and S. Kirkwood, "Tropopause fold occurrence rates over the Antarctic Station Troll (75 S, 2.5 E)," Ann. Geophys. **31** (4), 591–598 (2013).
11. K. Weigel, L. Hoffmann, G. Gunther, F. Khosrawi, F. Olschewski, P. Preusse, R. Spang, F. Stroh, and M. Riese, "A stratospheric intrusion at the subtropical jet over the Mediterranean Sea: Air-borne remote sensing observations and model results," Atmos. Chem. Phys. **12** (8), 8423–8438 (2012).
12. P. Pisoft, P. Sacha, L. M. Polvani, J. A. Anel, L. de la Torre, R. Eichinger, U. Foelsche, P. Huszar, C. Jacobi, J. Karlicky, A. Kuchar, J. Miksovsky, M. Zak, and H. E. Rieder, "Stratospheric contraction caused by increasing greenhouse gases," Environ. Res. Lett. **16** (6), 064038 (2021).
13. M. B. Follette-Cook, R. D. Hudson, and G. E. Nedoluha, "Classification of Northern Hemisphere stratospheric ozone and water vapor profiles by meteorological regime," Atmos. Chem. Phys. **9** (16), 5989–6003 (2009).
14. W. J. Collins, R. G. Derwent, B. Garnier, C. E. Johnson, M. G. Sanderson, and D. S. Stevenson, "Effect of stratosphere–troposphere exchange on the future tropospheric ozone trend," J. Geophys. Res. **108** (D12), 8528 (2003).

15. L. Geng, L. T. Murray, L. J. Mickley, P. Lin, Q. Fu, A. J. Schauer, and B. Alexander, "Isotopic evidence of multiple controls on atmospheric oxidants over climate transitions," Nature **546** (7656), 133–137 (2017).
16. P. J. Crutzen, "Albedo enhancement by stratospheric sulfur injections: A contribution to resolve a policy dilemma?," Clim. Change **77**, 211–219 (2006).
17. A. R. Ravishankara, "Water vapor in the lower stratosphere," Science **337** (6096), 809–810 (2012).
18. J. G. Anderson, D. M. Wilmouth, J. B. Smith, and D. S. Sayres, "UV dosage levels in summer: Increased risk of ozone loss from convectively injected water vapor," Science **337** (6096), 835–839 (2012).
19. R. Ueyama, E. J. Jensen, L. Pfister, G. S. Diskin, T. P. Bui, and J. M. Dean-Day, "Dehydration in the tropical tropopause layer: A case study for model evaluation using aircraft observations," J. Geophys. Res. Atmos. **119** (9), 5299–5316 (2014).
20. M. R. Schoeberl, H. B. Selkirk, H. Vomel, and A. R. Douglass, "Sources of seasonal variability in tropical upper troposphere and lower stratosphere water vapor and ozone: Inferences from the Ticosonde data set at Costa Rica," J. Geophys. Res. Atmos. **120** (18), 9684–9701 (2015).
21. C. Rolf, A. Afchine, H. Bozem, B. Buchholz, V. Ebert, T. Guggenmoser, P. Hoor, P. Konopka, E. Kretschmer, S. Muller, H. Schlager, N. Spelten, O. Suminska-Ebersoldt, J. Ungermann, A. Zahn, and M. Kramer, "Transport of Antarctic stratospheric strongly dehydrated air into the troposphere observed during the HALO-ESMVal campaign 2012," Atmos. Chem. Phys. **15** (16), 9143–9158 (2015).
22. V. F. Sofieva, J. Tamminen, E. Kyrola, T. Mielonen, P. Veefkind, B. Hassler, and G. E. Bodeker, "A novel tropopause-related climatology of ozone profiles," Atmos. Chem. Phys. **14** (1), 283–299 (2014).
23. I. Petropavlovskikh, E. Ray, S. M. Davis, K. Rosenlof, G. Manney, R. Shetter, S. R. Hall, K. Ullmann, L. Pfister, J. Hair, M. Fenn, M. Avery, and A. M. Thompson, "Low ozone bubbles observed in the tropical tropopause layer during the TC4 Campaign in 2007," J. Geophys. Res. **115**, J16 (2010).
24. P. Konopka and L. L. Pan, "On the mixing-driven formation of the extratropical transition layer (ExTL)," J. Geophys. Res. **117**, D18301 (2012).
25. B. Berchet, J.-D. Paris, G. Ancellet, K. S. Law, A. Stohl, Ph. Nedelec, M. Yu. Arshinov, B. Belan, and Ph. Ciais, "Tropospheric ozone over Siberia in spring 2010: Remote influences and stratospheric intrusion," Tellus B **65**, 19688 (2013).
26. C. R. Homeyer, K. P. Bowman, L. L. Pan, E. L. Atlas, R.-S. Gao, and T. L. Campos, "Dynamical and chemical characteristics of tropospheric intrusions observed during START08," J. Geophys. Res. **116**, D06111 (2011).
27. G. G. Anokhin, P. N. Antokhin, M. Yu. Arshinov, V. E. Barsuk, B. D. Belan, S. B. Belan, D. K. Davydov, G. A. Ivlev, A. V. Kozlov, V. S. Kozlov, M. V. Morozov, M. V. Panchenko, I. E. Penner, D. A. Pestunov, G. P. Sikov, D. V. Simonenkov, D. S. Sinitsyn, G. N. Tolmachev, D. V. Filippov, A. V. Fofonov, D. G. Chernov, V. S. Shamanaev, and V. P. Shmargunov, "OPTIK Tu-134 aicraft laboratory," Opt. Atmos. Okeana **24** (9), 805–816 (2011).
28. V. I. Otmakhov, E. V. Petrova, Z. I. Otmakhova, and T. V. Lapova, "Chemical and atomic–emission spectral analysis of atmospheric and industrial aerosols for the presence of base metals," Atmos. Ocean. Opt. **12** (4), 327–330 (1999).
29. B. D. Belan, G. A. Ivlev, A. V. Kozlov, T. M. Rasskazchikova, D. V. Simonenkov, and G. N. Tolmachev, "Typisation of the chemical composition of the tropospheric aerosol of the south of Western Siberia by the air mass," Proc. SPIE—Int. Soc. Opt. Eng. **10833**, 108338 (2018).
30. L. P. Golobokova, T. V. Khodzher, O. N. Izosimova, P. N. Zenkova, A. O. Pochyufarov, O. I. Khuriganowa, N. A. Onishyuk, I. I. Marinayte, V. V. Polkin, V. F. Radionov, S. M. Sakerin, A. P. Lisitzin, and V. P. Shevchenko, "Chemical composition of atmospheric aerosol in the Arctic region and adjoining seas along the routes of marine expeditions in 2018–2019," Atmos. Oceanic Opt. **33** (5), 480–489 (2020).
31. L. P. Golobokova, T. V. Khodzher, O. I. Khuriganova, I. I. Marinayte, N. A. Onishchuk, P. Rusanova, and V. L. Potemkin, "Variability of chemical properties of the atmospheric aerosol above Lake Baikal during large wildfires in Siberia," Atmosphere **11** (11), 1230 (2020).
32. A. R. Ivanova, "The tropopause: Variety of definitions and modern approaches to identification," Rus. Meteorol. Hydrol. **38** (12), 808–817 (2013).
33. M. J. Prather, X. Zhu, Q. Tang, J. Hsu, and J. L. Neu, "An atmospheric chemist in search of the tropopause," J. Geophys. Res. **116**, D04306 (2011).
34. A. R. Ivanova, "The tropopause slope as a characteristic of its deformation," Rus. Meteorol. Hydrol. **36** (2), 82–90 (2011).
35. S. P. Khromov, *Foundations for Synoptic Meteorology* (Gidrometeoizdat, Leningrad, 1948) [in Russian].
36. L. T. Matveev, *General Meteorology Course. Atmospheric Physics* (Gidrometeoizdat, St. Petersburg, 2000) [in Russian].
37. E. E. Remsberg, "Methane as a diagnostic tracer of changes in the Brewer–Dobson circulation of the stratosphere," Atmos. Chem. Phys. **15** (7), 3739–3754 (2015).
38. H. Bozem, P. Hoor, D. Kunkel, F. Köllner, J. Schneider, A. Herber, H. Schulz, W. R. Leaitch, A. A. Aliabadi, M. D. Willis, J. Burkart, and J. P. D. Abbatt, "Characterization of transport regimes and the polar dome during Arctic spring and summer using in situ aircraft measurements," Atmos. Chem. Phys. **19** (23), 15049–15071 (2019).
39. H. Oelhaf, B.-M. Sinnhuber, W. Woiwode, H. Bonisch, H. Bozem, A. Engel, A. Fix, F. Friedl-Vallon, J.-U. Grooß, P. Hoor, S. Johansson, T. Jurkat-Witschas, S. Kaufmann, M. Kramer, J. Krause, E. Kretschmer, D. Lorks, A. Marsing, J. Orphal, K. Pfeilsticker, M. Pitts, L. Poole, P. Preusse, M. Rapp, M. Riese, Ch. Rolf, J. Ungermann, Ch. Voigt, C. M. Volk, M. Wirth, A. Zahn, and H. Ziereis, "POLSTRACC," BAMS **100** (12), 2634–2664 (2019).
40. A. Volz, D. H. Enhalt, and R. G. Derwent, "Seasonal and latitudinal variations of ^{14}CO and the tropospheric

concentration of OH radicals," J. Geophys. Res. **86** (5), 5163–5171 (1981).

41. D. H. Enhalt, "The atmospheric cycle of methan," Tellus **26** (1), 58–70 (1974).
42. Q. Liang, J. M. Rodriguez, A. R. Douglass, J. H. Crawford, J. R. Olson, E. Apel, H. Bian, D. R. Blake, W. Brune, M. Chin, P. R. Colarco, A. Silva, G. S. Diskin, B. N. Duncan, L. G. Huey, D. J. Knapp, D. D. Montzka, J. E. Nielsen, S. Pawson, D. D. Riemer, A. J. Weinheimer, and A. Wisthaler, "Reactive nitrogen, ozone and ozone production in the Arctic troposphere and the impact of stratosphere-troposphere exchange," Atmos. Chem. Phys. **11** (24), 13 181–13 199 (2011).
43. C. Varotsos, J. Christodoulakis, C. Tzanis, and A. P. Cracknell, "Signature of tropospheric ozone and nitrogen dioxide from space: A case study for Athens, Greece," Atmos. Environ. **89**, 721–730 (2014)
44. L. S. Ivlev, *Chemical Composition and Structure of Atmospheric Aerosols* (Leningrad State Univ., Leningrad, 1982) [in Russian].
45. N. P. Shakina, I. N. Kuznetsova, and A. R. Ivanova, "Case studies of stratospheric intrusions associated with increased radioactivity in the surface air," Rus. Meteorol. Hydrol., No. 2, 38–43 (2000).
46. H.-M. Cho, Y. -L. Hong, and G. Kim, "Atmospheric depositional fluxes of cosmogenic 35S and 7Be: Implications for the turnover rate of sulfur through the biosphere," Atmos. Environ. **45** (25), 4230–4234 (2011).
47. T. Jurkat, S. Kaufmann, Ch. Voigt, D. Schauble, Ph. Jeßberger, and H. Ziereis, "The airborne mass spectrometer AIMS—Part 2: Measurements of trace gases with stratospheric or tropospheric origin in the UTLS," Atmos. Meas. Tech. **9** (4), 1907–1923 (2016).
48. J. Schneider, R. Weigel, T. Klimach, A. Dragoneas, O. Appel, A. Hünig, S. Molleker, F. Köllner, H.-Ch. Clemen, O. Eppers, P. Hoppe, P. Hoor, Ch. Mahnke, M. Krämer, Ch. Rolf, J.-U. Grooß, A. Zahn, F. Obersteiner, F. Ravegnani, A. Ulanovsky, H. Schlager, M. Scheibe, G. S. Diskin, J. P. Di Gangi, J. B. Nowak, M. Zöger, and S. Borrmann, "Aircraft-based observation of meteoric material in lower-stratospheric aerosol particles between 15 and 68_N," Atmos. Chem. Phys. **21** (2), 989–1013 (2021).